# ADVANCES IN MASSIVELY PARALLEL ELECTROMAGNETIC SIMULATION SUITE ACE3P*

Oleksiy Kononenko#, Lixin Ge, Kwok Ko, Zenghai Li, Cho-Kuen Ng, Liling Xiao
SLAC, Menlo Park, CA 94025, USA

*Abstract*

ACE3P is a 3D parallel electromagnetic simulation suite that has been developed at SLAC National Accelerator Laboratory for the past decades. Effectively utilizing supercomputer resources with advanced computational algorithms, ACE3P has become a unique modeling tool for the research and design of particle accelerators. Newly developed capabilities are presented, including the calculation of RF eigenmodes in large-scale accelerator structures using state-of-the-art scalable linear solvers, the enhanced multi-physics solutions for coupled electromagnetic, thermal and mechanical problems, the integration of ACE3P with the beam dynamics code IMPACT, as well as the interface of ACE3P to the particle-material interaction code Fluka for evaluating radiation effects in accelerators.

## INTRODUCTION

The ACE3P (Advanced Computational Electro- magnetics 3D Parallel) simulation suite has been developed at SLAC for the past decades consisting of modules in frequency and time domains for the research and design of particle accelerators [1]. This massively parallel set of codes is based on the finite-element method so that geometries of complex structures can be represented with high fidelity through conformal grids, and high solution accuracies can be obtained through high-order basis functions. Using high performance computing, ACE3P has provided a unique capability for large-scale simulations for the design, optimization and analysis of accelerating structures and systems. Running on DOE state-of-the-art supercomputers, parallel electromagnetics computation has enabled the design of accelerating cavities to machining tolerances and the analysis of accelerator systems to ensure operational reliability. The modeling effort has supported many of the accelerator projects within the DOE accelerator complex and beyond such as LHC upgrade and PIP-II, CEBAF upgrade, FRIB and e-RHIC, as well as LCLS and LCLS-II at SLAC [2,3].

ACE3P consists of the following modules:

- Omega3P, an electromagnetic eigensolver;
- S3P, a frequency-domain S-parameter solver;
- T3P, a time-domain solver for transients and wakefield computations;
- Track3P, a particle tracking code for multipacting and dark current studies;
- Pic3P, a particle-in-cell code for self-consistent particle and field interactions;
- TEM3P, a multi-physics code for integrated electromagnetic, thermal and mechanical effects.

A typical ACE3P simulation workflow also includes preprocessing of model and mesh building in Cubit [4] as well as post-processing results in Paraview [5], see Fig. 1. While preprocessing and postprocessing procedures can be both performed on a local desktop, ACE3P solvers run on supercomputers at the National Energy Research Scientific Computing Center (NERSC) [6], which is a major facility for scientific computing in the US.

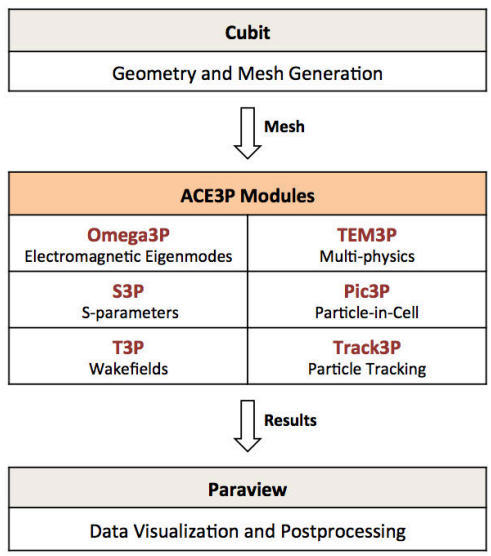


Figure 1: A typical simulation workflow for ACE3P.

Recent advances in the development and application of ACE3P include

- State-of-the-art hybrid linear solver [7] implementation in Omega3P for fast electromagnetic eigenmodes analysis;
- Accurate determination of temperature distribution for realistic 3D accelerator components using the thermal solver in TEM3P [8];
- Development of an eigensolver in TEM3P to determine mechanical modes of a superconducting (SRF) cavity facilitating the investigation of microphonics [9];
- Development of a harmonic response solver in TEM3P to calculate damped and undamped mechanical responses of an SRF cavity to external harmonic excitations [10];
- Development of an electro-mechanical analysis tool to decompose structural displacements into those of the mechanical modes of an SRF cavity required for

*Work supported by DOE Contract No. DE-AC02-76SF00515
#Oleksiy.Kononenko@slac.stanford.edu

ISBN 978-3-95450-136-6

the design of feedback control loop ensuring operational reliability of particle accelerator;
- Integration of the ACE3P suite with the beam dynamics code IMPACT-T [11] for realistic calculations of beam emittance in accelerators;
- Interface of ACE3P to the particle-material interaction code Fluka [12] for evaluating radiation effects.

The corresponding simulation results are presented in the following sections in details.

## IMPLEMENTATION OF HYBRID LINEAR SOLVER IN ACE3P

In collaboration with Lawrence Berkeley National Laboratory, the parallel domain decomposition Schur complement based linear solver (PDSLin) [7] was implemented in ACE3P's eigensolver Omega3P and applied to calculate higher-order modes (HOMs) in the Project X (and later PIPI-II) 650 MHz cryomodule [13]. Compared with direct solvers, the hybrid linear solver PDSLin uses less memory per core per run, and hence can utilize most of the resources in a NERSC compute node. The monopole HOMs above the beampipe cutoff calculated using PDSLin in Omega3P are shown in Fig. 2. It took about 3 minutes to calculate each mode using 300 cores in 25 nodes and a total of 1.1 TB of memory on NERSC Edison supercomputer.

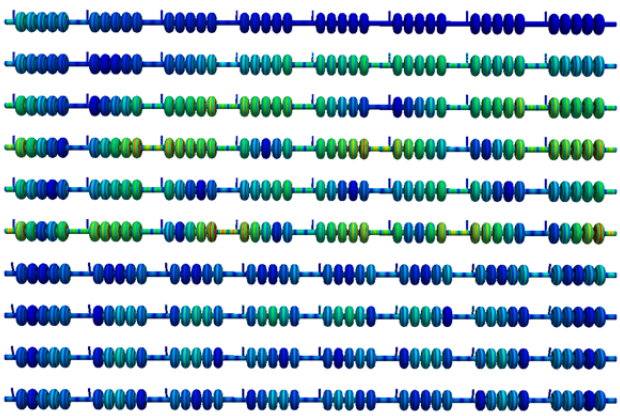

Figure 2: HOMs in Project X 650 MHz cryomodule.

In comparison, a similar calculation, performed several years ago, took about 1 hour per mode on NERSC Seaborg system using the direct solver MUMPS [14]. On average, the memory usage per process for PDSLin is five times less than MUMPS, allowing the solution of large problem sizes that cannot be handled by direct solvers.

## THERMAL CALCULATIONS FOR LCLS-II COUPLER

The LCLS-II project [15] at SLAC National Accelerator Laboratory adopts the TTF3 coaxial fundamental power coupler (FPC) with modest modifications to make it suitable for continuous-wave operation. The coupler consists of a cold and a warm sections made of different types of materials with a thin copper coating at the warm side. The fully 3D geometry of the coupler is simulated using TEM3P to determine the temperature distribution along the feedthrough of the coupler [8].

First, electromagnetic fields are calculated in the FPC vacuum and ceramic regions using S3P. Then, the corresponding power losses on the metal walls as well as in the ceramic window are used as the heat load input for TEM3P thermal simulation. The RF and thermal models share a common geometrical interface, so that the heat flux information can be easily converted into the proper boundary condition, see Fig. 3.

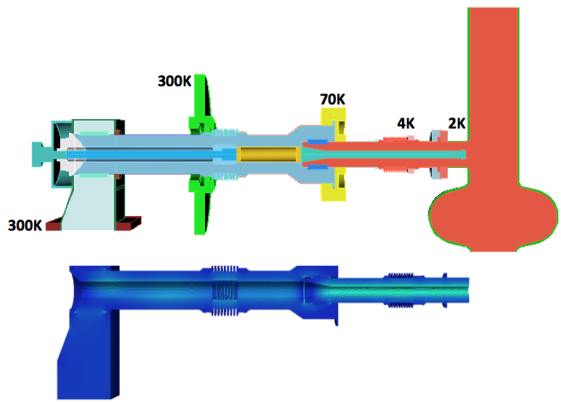


Figure 3: FPC model for TEM3P thermal simulation (top) and RF field distribution calculated with S3P in the vacuum/ceramic regions (bottom).

The temperature distribution shown in Fig. 4 is obtained using 6 kW power for the standing wave on resonance. The maximum temperature is found at the bellows near the central region of the coupler (red zone in Fig. 4) and agrees well with the value from high power tests at Fermilab [16], as shown in Fig. 5.

Fully 3D analysis is essential here as the 2D COMSOL desktop simulations (green and blue curves in Fig. 5) have both discrepancies compared to the measured data and significantly underestimated the maximum temperature.

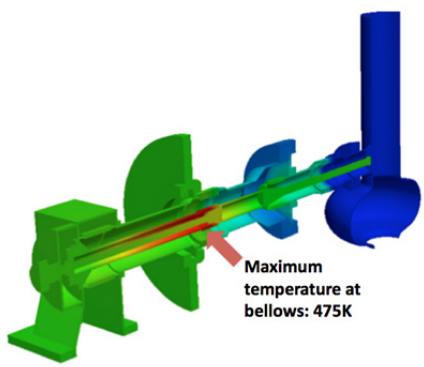


Figure 4: Temperature distribution in TTF3 coupler calculated using TEM3P.



ISBN 978-3-95450-136-6

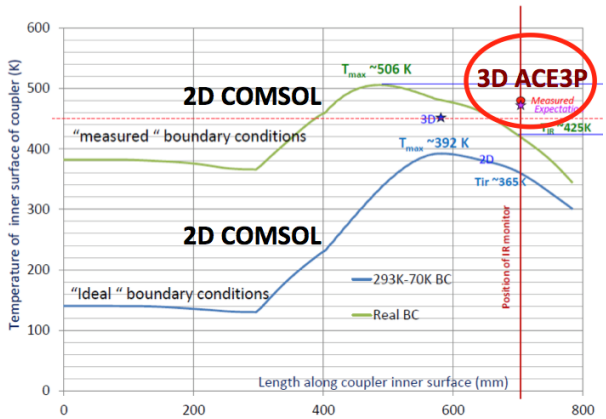


Figure 5: Temperature along the inner conductor with the red dot showing the agreement of ACE3P simulation and measurement (Courtesy of A. Hocker, Fermilab).

The simulation has been made feasible by the availability of shell elements in TEM3P, which enables the modeling of the thin copper coating on the conductor wall without the use of extremely small elements. In addition, 3D parallel computation through the use of multiple processors allows for high-resolution simulation by taking advantages of large memory resources and speedup.

## ELECTRO-MECHANICAL SIMULATIONS FOR SRF CAVITY

RF fields in superconducting accelerating structures exert pressure upon all the surfaces exposed to electromagnetic radiation. Unless carefully studied and controlled, it may significantly affect the operational reliability of a particle accelerator. To mitigate this adverse effect (Lorentz force detuning) a corresponding feedback loop must be developed to tune the cavity during the operation.

Equation (1) describes how the cavity RF frequency is affected by a particular mechanical mode excited by the the changes in field amplitude and/or external noise sources [17].

$$\Delta\ddot{\omega}_\mu + \frac{2}{\tau_\mu}\Delta\dot{\omega}_\mu + \Omega_\mu^2\Delta\omega_\mu = -k_\mu\Omega_\mu^2 V(t)^2 + n(t). \quad (1)$$

where $\Delta\omega_\mu$ is an RF circular frequency shift due to a μ-th mechanical mode, $\tau_\mu$ is the mode decay time, $\Omega_\mu$ is the mechanical eigenfrequency, $k_\mu$ is the coupling coefficient between the RF field and mechanical mode $\mu$, $V(t)$ is the accelerating voltage and $n(t)$ is a driving term due to external vibrations or microphonics.

### *Mechanical Eigenmode Calculations*

To determine the mechanical eigenmodes of the LCLS-II SRF TESLA cavity, an eigensolver has been developed in TEM3P [9]. In Fig. 6 the simulation model for the TEM3P mechanical calculation is shown for the TESLA cavity positioned in a helium tank.

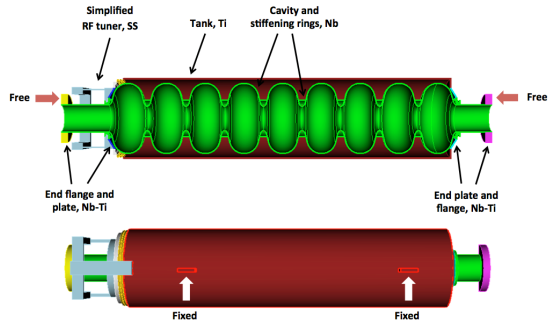


Figure 6: Simulation model for the TEM3P mechanical calculation of the TESLA cavity in a Helium tank.

A fully 3D eigenmode calculation involving multiple materials was performed to determine dressed cavity eigenfrequencies. Table 1 shows that they are in good agreement with the dominating modes determined in measurements [18-19].

Table 1: Eigen Frequencies of the Dressed TESLA Cavity Calculated Using ACE3P and Measured at Fermilab

| ACE3P | Measurement | Strength |
|---|---|---|
| 233 | 235 | 0.65 |
| 176 | 168 | 0.1 |
| 473 | 471 | 0.09 |

### *Electro-Mechanical Simulations*

The determination of Lorentz force detuning requires a coupled electro-mechanical calculation, where the electromagnetic field is first calculated using Omega3P in the vacuum region of the cavity and then the Lorentz force on the cavity surface serves as the boundary condition for TEM3P to determine deformations of the cavity wall. For simplicity and demonstration purposes we consider a model of the undressed SRF cavity in the following calculations.

Figure 7 shows the Lorentz force displacement for the TESLA structure using an accelerating gradient of 16 MV/m, with a free and a fixed boundary condition imposed on the left and the right ends of the cavity, respectively. The displacement is largest at the free end and falls off gradually towards the fixed end.

Figure 7: Lorentz force displacement of the TESLA cavity using a quarter model of the geometry.

Using TEM3P's mechanical eigensolver, the first three eigenmodes for the quarter model subject to the same boundary constraints are shown in Fig. 8. Because of the boundary conditions imposed on the symmetry planes, only longitudinal modes are modeled.

The coupling of Lorentz force displacement to individual mechanical modes is computed by a modal decomposition. In this regard, the displacement shown in Fig. 7 is expressed as a linear combination of a complete set of displacements from the orthogonal modes, three of those are shown in Fig. 8:

ISBN 978-3-95450-136-6

$$\vec{u}(x,y,z)=\sum_{\mu=0}^{\infty} q_\mu \vec{u}_\mu(x,y,z)$$

where $q_\mu$ is the coupling cofficient of the $\mu$-th mechanical mode, from which one can determine the contribution to the frequency shift by this mode if it is excited.

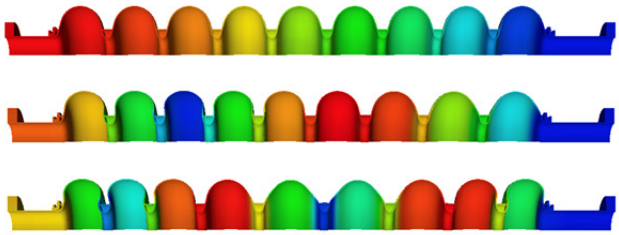

Figure 8: Mechanical modes of the TESLA cavity with frequencies 96 Hz, 296 Hz and 496 Hz (from top to bottom).

Assuming a specific accelerating voltage V, the Lorentz force coefficient $k_\mu$ for the $\mu$-th mechanical mode is calculated as

$$k_\mu = \frac{\Delta f_\mu^{RF}}{V^2}.$$

Table 2: Lorentz Force Coefficients for the Ten Lowest Mechanical Modes of the LCLS-II SRF Cavity

| Mode | Ω[Hz] | q | $\Delta f^{RF}$[Hz] | k [Hz/MV$^2$] |
|---|---|---|---|---|
| 1 | 99 | -4.8E-06 | -930 | -2.21 |
| 2 | 297 | 7.51E-07 | -145 | -0.34 |
| 3 | 497 | 3.38E-07 | -43 | -0.1 |
| 4 | 695 | 2.59E-07 | -36 | -0.09 |
| 5 | 890 | 1.91E-07 | -15 | -0.04 |
| 6 | 1075 | 1.68E-07 | -18 | -0.04 |
| 7 | 1246 | 1.37E-07 | -6 | -0.01 |
| 8 | 1393 | 1.22E-07 | -10 | -0.02 |
| 9 | 1493 | 6.03E-08 | 0 | 0 |
| 10 | 1585 | 2.65E-07 | -33 | -0.08 |
| **Total** | – | – | **-1236** | **-2.93** |
| **Static LF** | – | – | **-1192** | **-2.83** |

Table 2 lists the decomposition of the Lorentz force displacement into the first ten longitudinal modes. It can be seen that the major contributions to the total RF frequency shift are from the several lowest mechanical modes and the summation of $\Delta f_i^{RF}$ by them is very close to the value of static Lorentz force.

The eigenfrequencies and k-coefficients of the mechanical eigenmodes will provide useful information for studying microphonics effects using a feedback control algorithm [20] based on Eq. (1).

## INTEGRATION OF ACE3P AND IMPACT

IMPACT-T[ 11] is a parallel, 3D space-charge tracking code to study beam dynamics in photo-injectors and linear accelerators. The code can track particles using its built-in beamline element models, or using the external field maps of beamline elements provided by users for more accurate modeling of 3D effects.

Integrating ACE3P with IMPACT-T presents a new parallel capability that combines 3D electromagnetic simulation with beam dynamics calculation so that accelerator cavities and beamline elements can be modeled on a system scale with high accuracy. The representations of field data (in terms of 3D and transfer maps) in the two simulation software packages have been standardized to enable the transfer of cavity RF fields from ACE3P to IMPACT-T for particle tracking.

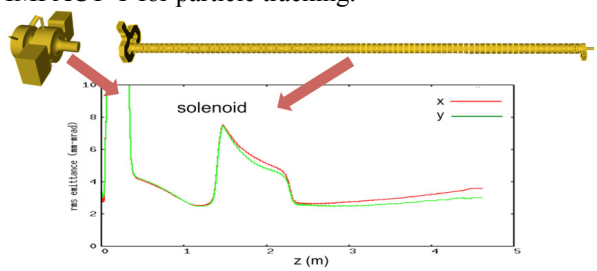


Figure 9: Beam emittances in the transverse directions as a function of the longitudinal position for the FACET-II injector (Courtesy of J. Qiang, LBNL).

The beam emittances in the transverse directions calculated by the integrated simulation as a function of the longitudinal position for the FACET-II injector, which includes an RF gun, an S-band accelerating structure and a solenoid between them, are shown in Fig. 9. The electromagnetic fields of the accelerating modes of the RF gun and the accelerating structure to produce the respective 3D field maps are calculated using Omega3P and then read into IMPACT-T for particle tracking of a low energy beam using the field maps for the full length of the injector. This integrated simulation at the system scale has been performed using the NERSC supercomputers.

## INTERFACE OF ACE3P TO RADIATION CALCULATION

Accelerator cavities operating at high gradients are subject to damage from high-energy electrons hitting the surface of the cavity wall. These electrons are believed to originate from certain locations of the cavity surface due to field emission, and then accelerated under the RF field before impacting the cavity wall. Interacting with the certain materials, they produce electromagnetic radiation that can affect the performance of the accelerator. For instance, during the commissioning of cryomodule at Jefferson Lab, strong radiation dosages along the cryomodules were observed during the processing period, regardless of the presence of the beam [21].



ISBN 978-3-95450-136-6

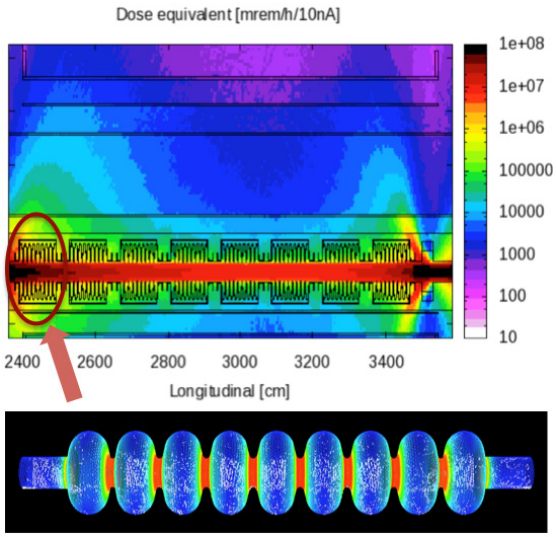


Figure 10: The radiation dose for the LCLS-II cryomodule as calculated in Fluka (top) and a snapshot of the electron distribution in the coupled Track3P calculation for one SRF cavity (top) (Courtesy of M. Santana, SLAC).

ACE3P provides simulation modules that model the 3D electromagnetic fields in an accelerator cavity (Omega3P, S3P and T3P), generate the initial field emission electrons and track the electrons in the vacuum region of the cavity (Track3P). When the electrons hit the surface of the cavity wall, their phase space information are transferred to the particle-material interaction code Fluka [12] for radiation calculation.

Figure 10 shows the calculation of the radiation dose for the LCLS-II cryomodule. Track3P is used to simulate dark current in a LCLS-II cavity, and an interface has been developed to transfer particle data on the cavity surface from Track3P to Fluka to calculate radiation produced by the interaction of the electrons with the wall materials [22].

## CONCLUSIONS

Under SLAC and DOE SciDAC [23] program support, new modeling capabilities have been developed in ACE3P in recent years and successfully benchmarked against measurements. Through high performance computing, simulation using ACE3P has enabled the solution of challenging computational problems for a wide range of applications in accelerator projects, accelerator science and development. With ongoing development and enhancement of its multi-physics capabilities including integration with other accelerator codes and implementation of state-of-the-art scalable numerical algorithms, ACE3P can be used to facilitate optimized accelerator design and reliable machine operation, thus reducing costs and saving time.

## ACKNOWLEDGEMENTS

We would like to thank A. Hocker, J. Qiang and M. Santana for collaborations. This research used resources of the National Energy Research Scientific Computing Center, which is supported by the Office of Science of the U.S. Department of Energy under Contract No. DE-AC02-05CH11231.

## REFERENCES

[1] Massively parallel electromagnetic ACE3P Simulation Suite, https://portal.slac.stanford.edu/sites/ard_public/acd/
[2] K. Ko et al., "Advances in Parallel Computing Codes for Accelerator Science and Development," Proc. LINAC2010, Tsukuba, Japan, 2010.
[3] L. Ge, K. Ko, O. Kononenko, Z. Li, C.-K. Ng, L. Xiao, "Advances In Parallel Finite Element Code Suite ACE3P,"
[4] " Proc. IPAC15, Richmond, VA, USA May 3-8, 2015.
[5] The CUBIT Geometry and Mesh Generation Toolkit, https://cubit.sandia.gov/
[6] Paraview, http://www.paraview.org/
[7] National Energy Research Scientific Computing Center, https://www.nersc.gov/
[8] I. Yamazaki, PDSLin User Guide, 2012.
[9] L. Xiao et al., "TTF Power Coupler Thermal Analysis for LCLS-II CW Application," Proc. IPAC15, Richmond, USA, 2015.
[10] O. Kononenko et al., "A Massively Parallel Finite-Element Eigenvalue Solver for Modal Analysis in Structural Mechanics," Technical Report SLAC-PUB-16229, SLAC, 2014.
[11] O. Kononenko, "A Massively Parallel Solver for Mechanical Harmonic Analysis of Accelerator Cavities," Technical Report SLAC-PUB-15976, SLAC, 2015.
[12] IMPACT-T: A 3D Parallel Particle Tracking Code in Time Domain, Official webpage, http://amac.lbl.gov/~jiqiang/IMPACT-T/index.html
[13] Fluka, https://www.fluka.org/
[14] A. Saini, et al., Design of Superconducting CW Linac for PIP-II, Proc. IPAC15, Richmond, USA, 2015, pp. 565-567.
[15] M. Paszyński, D. Pardo, A. Paszyńska, "Parallel multi-frontal solver for p adaptive finite element modeling of multi-physics computational problems," Journal of Computational Science, 1(1), 2010. pp. 48-54.
[16] Linac Coherent Light Source II, Official web page, https://portal.slac.stanford.edu/sites/lcls_public/lcls_ii/Pages/default.aspx
[17] A. Hocker, "LCLS-II Coupler Test Results," FNAL presentation, 2014.
[18] J. Delayen, Ponderomotive instabilities and microphonics–a tutorial, Proceedings of the 12th International Workshop on RF Superconductivity, Cornell University, Ithaca, New York, USA.
[19] W. Schappert et al., "Resonance Control for Narrow-Bandwidth, Superconducting RF Applications," Proc. SRF2015, Whistler, Canada, 2015.
[20] Y. Pischalnikov et al., "Design and Test of Compact Tuner for Narrow Bandwidth SRF Cavities," Proc. IPAC15, Richmond, USA, 2015.
[21] Z. Li et al., "Multi-Physics Analysis of CW Superconducting Cavity for the LCLS-II Using ACE3P," Proc. IPAC14, Dresden, Germany, 2014.
[22] F. Marhauser et al., "Field Emission and Consequences as Observed and Simulated for CEBAF Upgrade Cryomodules," Proc. of SRF 2013, Paris, Sep 23-27, 2013.
[23] C. Adolphsen, "High Power RF Status," LCLS-II DOE Review, April 7-9, 2015, SLAC.
[24] DOE SciDAC, http://www.scidac.gov/

ISBN 978-3-95450-136-6